Apparent viscosity and cortical tension of blood granulocytes determined by micropipet aspiration

E. Evans and A. Yeung
Departments of Pathology and Physics, University of British Columbia, Vancouver, British Columbia, Canada V6T 1W5

ABSTRACT Continuous deformation and entry flow of single blood granulocytes into small caliber micropipets at various suction pressures have been studied to determine an apparent viscosity for the cell contents and to estimate the extent that dissipation in a cortical layer adjacent to the cell surface contributes to the total viscous flow resistance. Experiments were carried out with a wide range of pipet sizes (2.0–7.5 μm) and suction pressures (10^2–10^4 dyn/cm^2) to examine the details of the entry flow. The results show that the outer cortex of the cell maintains a small persistent tension of ~0.035 dyn/cm. The tension creates a threshold pressure below which the cell will not enter the pipet. The superficial plasma membrane of these cells appears to establish an upper limit to surface dilation which is reached after microscopic "ruffles" and "folds" have been pulled smooth. With aspiration of cells by small pipets (<2.7 μm), the limit to surface expansion was derived from the maximal extension of the cell into the pipet; final areas were measured to be 2.1 to 2.2 times the area of the initial spherical shape. For suctions in excess of a threshold, the response to constant pressure was continuous flow in proportion to excess pressure above the threshold with only a small nonlinearity over time until the cell completely entered the pipet (for pipet calibers >2.7 μm). With a theoretical model introduced in a companion paper, (Yeung, A., and E. Evans. 1989. *Biophys. J.* 56:139–149) the entry flow response versus pipet size and suction pressure was analyzed to estimate the apparent viscosity of the cell interior and the ratio of cortical flow resistance to flow resistance from the cell interior. The apparent viscosity was found to depend strongly on temperature with values on the order of 2×10^3 poise at 23°C, lower values of 1×10^3 poise at 37°C, but extremely large values in excess of 10^4 poise below 10°C. Because of scatter in cell response, it was not possible to accurately establish the characteristic ratio for flow resistance in the cortex to that inside the cell; however, the data showed that the cortex does not contribute significantly to the total flow resistance.

INTRODUCTION

Micropipet aspiration (1) of passive blood granulocytes has shown that the response is continuous liquid-like flow for suction pressures in excess of a threshold. The aspirated projection of cells inside pipets at constant suction pressures of 10^2–10^4 dyn/cm^2 increase linearly or slightly nonlinearly, but very slowly over time. In order to produce flow, suction must exceed threshold pressure levels on the order of 10^2 dyn/cm^2. For pipet calibers larger than 2.7 μm, cells are totally aspirated after times that range from seconds to minutes in inverse proportion to the aspiration pressure. Flow of these cells into small pipets leads to extensions that are several fold larger than the undeformed cell diameter. If the suction pressure is lowered to the threshold value during an experiment, flow ceases; when the cell is released from the pipet, the cell slowly recovers its initial spherical form. The liquid-like response of granulocytes to constant suction pressures is also consistent with the nearly spherical geometries observed for the cell segment exterior to the pipet during aspiration and the perfect spherical form of the passive cell after recovery from large deformations. Collectively, the observations indicate that the cell behaves like a highly viscous liquid drop with a persistent cortical tension. Furthermore, the viscous-liquid nature of the cell interior has been verified and quantitated with clever "magnetic depolarization" experiments (2). Continuous flow observed at moderate to high suction pressures is in contrast to the small quasi-static deformation observed close to the threshold pressure or for short pressure pulses which has been studied extensively by other investigators (3, 4).

Mechanical response is only one factor to consider in the development of a material model for cell deformation. Biochemical and ultrastructural characteristics must also be considered. Here, evidence indicates that, in addition to the organellar constituents (e.g., nucleus, granules, etc.) inside the cell, there is a cortical layer adjacent to the cell plasma membrane which includes much of the con-

Address correspondence and reprint requests to E. Evans.

0006-3495/89/07/151/10 $2.00

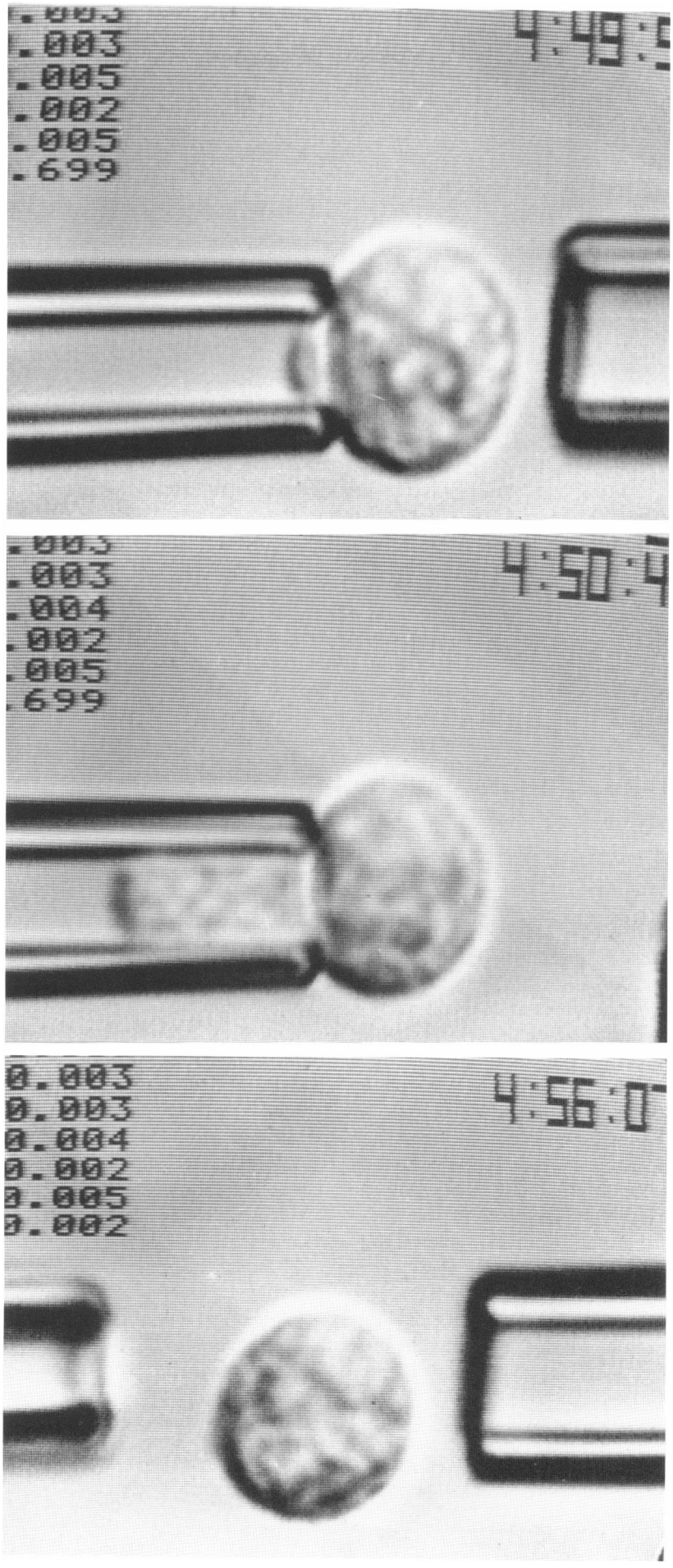
.003
.005
.002
.005
.699
4:49:5
.003
.003
.004
.002
.005
.699
4:50:4
0.003
0.003
0.004
0.002
0.005
0.002
4:56:0

tractile apparatus for phagocytes like granulocytes, monocytes, and macrophages (5–8). The contractile matrix is formed by polymerization of actin filaments through actin-binding proteins in association with myosin (8). The contractile layer is likely the source for persistent tension. This subsurface matrix may also possess significant viscous characteristics that could contribute to the passive resistance of the cell to deformation. Together, the mechanical response observed in pipet suction experiments and this chemical-structural evidence have led us to examine a particular mechanical model for passive deformation of liquid-like spherical cells: i.e., a viscous liquid core encapsulated by a distinct cortical layer.

In a companion paper (9), we examined the behavior expected for flow of the model cell into pipets as a function of suction pressure, pipet size, and a characteristic ratio for flow resistance in the cortex to that of the liquid core. The response was found to be scaled by pipet dimension in different ways as viscous contributions from the interior liquid core and the cortical layer were varied. To examine the merits of this analysis and to derive estimates of effective viscosity for phagocytes (e.g., granulocytes), we have carried out extensive entry flow tests on single granulocytes with pipet sizes chosen over as large a range as technically feasible. Further, multiple tests on individual cells were performed to minimize cell-to-cell variations. In these experiments two different size pipets were used to aspirate a single cell and two different levels of suction pressure were applied with each pipet. The suction pressures were chosen as integral multiples of the threshold pressure determined initially with each pipet. In previous studies (1), we examined the extent of flow measured by the projection length inside the pipet after a 60 s exposure to suction pressure and found it to be essentially proportional to the applied pressure with increased rates for larger pipet sizes. Because of the small number of cells tested in the earlier experiments for each pipet size and the large variation in response from cell-to-cell, it was difficult to establish the functional behavior of the entry flow; thus, these additional tests have been carried out to more critically examine the passive flow response of granulocytes as a function of pipet diameter and suction pressure. As we will show, correlation of the measured resistances to flow (excess pressure above the threshold divided by rate of entry into pipets) with the cortical shell-liquid core model yields values of apparent viscosity for granulocytes equal to the values obtained previously by Valberg and Feldman (2) using magnetic particle methods and lung macrophages.

FIGURE 1 Sequence of video micrographs of a blood granulocyte aspirated into a 3.5 μm caliber pipet: (*a*) first, formation of a hemispherical cap at the threshold pressure with no further flow; (*b*) next, the extent of flow after the suction was elevated above the threshold for a fixed time period then returned to the threshold value; and (*c*) recovery of the cell to its initial spherical form after release from the pipet.

METHODS

Granulocytes to be tested in micromechanical experiments were obtained from fresh blood samples by finger-prick from a single donor. These cells were immediately suspended in a phoshpate buffered saline solution with 10% compatible plasma, then injected into a small microchamber on the microscope stage. Cell experiments were carried out over a period from 5 to 40 min and the results exhibited no dependence on the residence time in the chamber. Plasma was separated from whole blood samples collected in 10 mM sodium citrate anticoagulant, centrifuged at 8,000 *g* for 4 min; the supernatant plasma was removed and filtered for use in the experiment. We have found previously that plasma at concentrations greater than or equal to 10% mixed with the suspending buffer prevented adhesion of the granulocytes to the pipet wall (1). Also, when the calcium concentration in the solution was at or above the value ($\sim 10^{-6}$ M) established by sodium citrate, passive deformation of granulocytes was found to be independent of calcium level whereas further reduction in calcium (as in EDTA or EGTA buffers) resulted in an increase in the threshold pressure for initiation of cell flow. Granulocytes were selected at random from the very low hematocrit samples in the microchamber with the use of a differential interference contrast optical system. Identification of granulocytes was based on the observation of small size, densely packed granules within the cell and (as best as could be detected) a lobulated nucleus. The sizes of granulocytes selected by this procedure fell into a narrow range of 8–9 μm in diameter.

Deformation tests on single granulocytes were performed by micropipet aspiration; the procedure involved three pipets: two pipets for separate entry tests and a third pipet to convey the granulocyte into position for rapid aspiration by one of the test pipets. Suction pressures in the test pipets ranged from 10^2 to 10^4 dyn/cm^2. To begin the test, suction pressure in one pipet was increased until the cell projection inside the pipet would just exceed a pipet radius but without further flow. This provided a measure of the threshold pressure. Next, the pressure was increased by a step (in <0.1 s) to a constant multiple value of the threshold, held for a period sufficient to produce large projections inside the tube, and then returned to the initial value obtained for the threshold. Finally, the cell was released and allowed to recover its initial spherical shape before it was subjected to the next test with another pressure and/or the second test pipet of a different size. Progress of the experiment was recorded on video tape; video micrographs of a single cell response to the pipet suction history just described are shown in Fig. 1. Data analysis for each test involved measurement of the cell segment dimension exterior to the pipet and projection length inside the pipet throughout the aspiration test. As noted in previous studies (1), occasionally cells became active during an aspriation test as evidenced by erratic length changes in the pipet or pseudopod formation on the exterior surface. Activation occurred late in an aspiration test or not at all; active cells were excluded from consideration in the data analysis. Pipet sizes were chosen in a range from 2.0 to 7.5 μm; pipet calibers were determined from the insertion depth of a microneedle that had been calibrated with the use of a scanning electron microscope. Pressures were recorded through continuous water manometer systems to sensitive digital pressure transducers with a resolution of a microatmosphere (dyn/cm^2). Cell tests with one pipet were carried out over a range of temperatures from 10° to 37°C; multiple pipet tests on individual cells were performed only at room temperature (23°C).

ANALYSIS AND RESULTS

As observed previously (1), suction had to exceed a threshold pressure to initiate granulocyte flow into a pipet. This threshold pressure was measured as outlined in the Methods section with various pipet sizes. Fig. 2 shows a plot of the experimental values of pressure threshold and the theoretical correlation based on the presence of a persistent tension $\bar{\tau}_o$ in the cell cortex. Threshold predictions were derived with the tension and the pressure required to establish a static hemispherical projection inside the pipet as given by,

$$P_{cr} = 2\bar{\tau}_o(1/R_P - 1/R_c).$$

R_P and R_c are the radii of the suction pipet and the outer spherical segment of the cell, respectively. From the correlation shown in Fig. 2, the average cortical tension for passive granulocytes was found to be $\bar{\tau}_o = 0.035$ dyn/cm. Cortical tension appears to account for the spherical shapes of liquid-like cells in suspension and for the driving force that leads to recovery after deformation.

When suction was increased above the threshold, cells flowed continuously into pipets to an extent determined by pipet caliber. With pipet calibers smaller than 2.7 μm, the fixed area of the superficial plasma membrane eventually limited the extent of aspiration when microscopic ruffles and folds were pulled smooth. Extension beyond this point required very large suction pressures and led to lysis after only a small displacement. Fig. 3 shows video micrographs of an undeformed spherical cell and the same cell maximally extended into a small pipet. Measurements of the ultimate projection length inside small pipets and the diameter of the exterior spherical segment outside the pipet were used to calculate the total area and volume of the maximally deformed cell. From these measurements, we found that the volume remained equal (within an experimental resolution of 5%) to the initial volume of the undeformed spherical cell. However, the surface areas of maximally extended cells were 2.1–2.2 times the projected areas of the ruffled membrane surface in the initial spherical form (increases in projected area of 110 to 120%). These direct measurements of excess area in ruffles are slightly larger than the value of 84% estimated by morphometric methods (10). By comparison, aspiration into pipets larger than 2.7 μm led to total aspiration of granulocytes with any pressure in excess of the threshold which demonstrated that the cells behaved as liquid-like bodies.

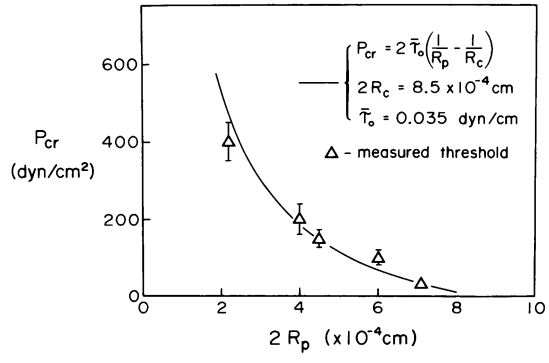

FIGURE 2. Threshold pressures required to form initial hemispherical projections inside pipets without further flow versus pipet radii. The solid curve is the theoretical correlation based on the presence of a persistent tension $\bar{\tau}_o = 0.035$ dyn/cm in the cell cortex. The average cell diameter was measured to be 8.5 μm.

To minimize variations from cell-to-cell, four entry flow tests were done on each cell using two pipets with different diameters; the cell was aspirated into each pipet with two different levels of excess pressure. Between tests, the cell was allowed to fully recover its spherical shape. At the beginning of each test, the threshold pressure was determined for the particular pipet; the suction pressure was then increased to an integral-multiple of the threshold and held fixed for a period of time sufficient to yield aspiration lengths of 3 to 6 pipet radii. Finally, pressure was reduced to the initial threshold level and held constant for a period of time that allowed any transient recovery of extension inside the pipet to be observed. Fig. 4 shows the sequence and results for projection length versus time for a single granulocyte subjected to three aspiration tests with one pipet where suction pressures were 1.5–4.3 times the threshold value. The rationale behind the choice of four tests was first of all to determine whether or not the mechanical response represented a Newtonian flow where rate of entry into the pipet is proportional to the excess pressure and secondly to examine the extensive size-dependence of the entry flow rate on pipet caliber. As shown in a companion paper (9), the rate of entry is scaled by the excess pressure,

$$\mu(\dot{L}/R_p)/[\Delta P - P_{cr}] = f(R_p/R_c, \tilde{\eta})$$

to yield a function that only depends on pipet size for ideal Newtonian properties. In fact, excess pressure scaled by the rate of entry is directly proportional to the apparent viscosity μ of the cell contents.

As shown in Fig. 4, each test was characterized by three consistent responses: (*a*) When suction was maintained at P_{cr}, the initial hemispherical cap was formed inside the pipet with no further flow. (*b*) When suction was stepped to a higher value, entry flow was continuous (often slightly nonlinear) never indicating an approach to static equilibrium. (*c*) Finally, when suction was returned to the threshold level, flow ceased with an occasional

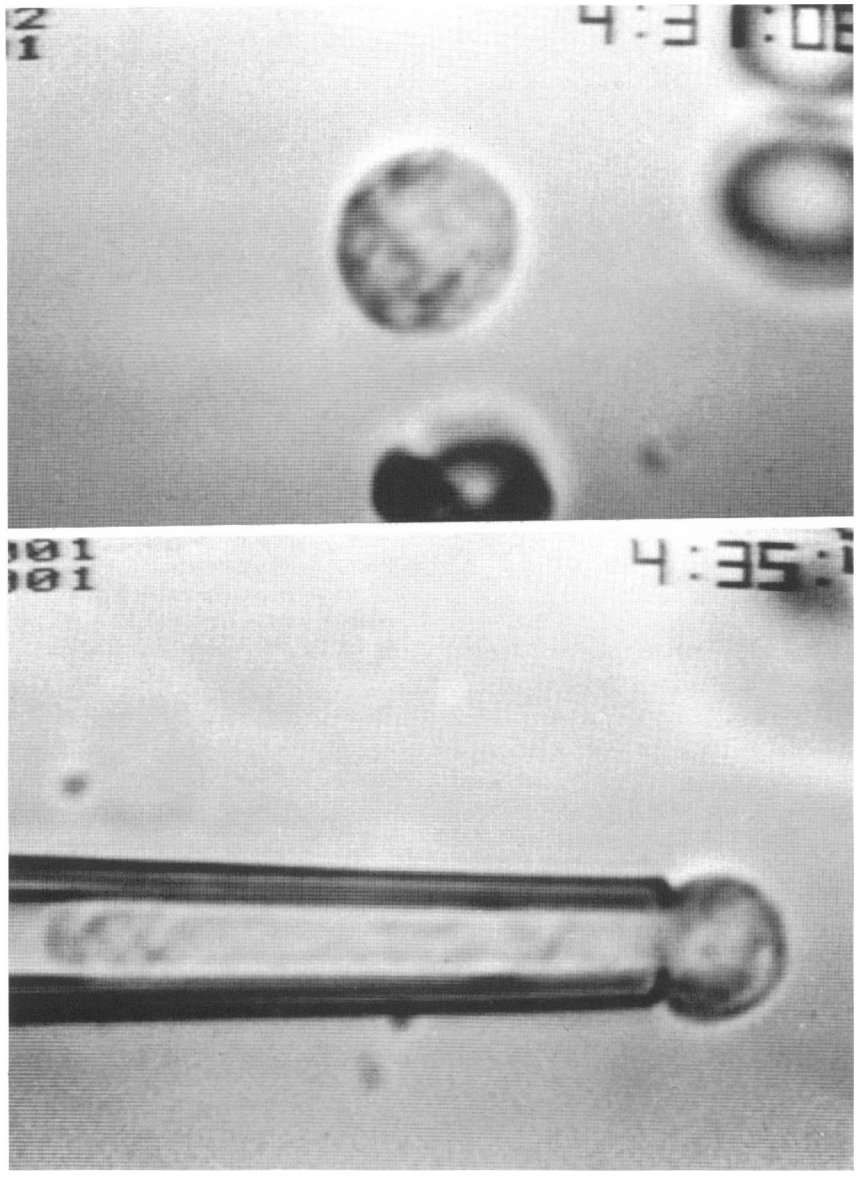

FIGURE 3. Video micrographs of a spherical granulocyte before and after aspiration into a small micropipet to maximum extension (lysis would occur if displaced further). This illustrates the redundancy of the plasma membrane envelope which was found to be on the order of 2.1–2.2 times the projected area of the ruffled spherical form. (Note: the magnification here was about ⅔ of that used for Fig. 1.)

small recoil in the projection length but no further movement. Observations of small projection length recoil and slight nonlinearity in flow over time are departures from ideal liquid behavior. These subtle deviations could be modeled by modification of the ideal liquid behavior to include a small fading elastic component parallel with the primary viscous response. However, these deviations were sometimes absent, clearly not dominant features of the flow, and thus can be considered as secondary effects in the rheological description of granulocyte flow at these pressures. Therefore, we focus on the principal liquid-like property exhibited by the entry flow.

For each observation of projection length versus time, an average rate of entry was determined by fitting two straight lines to the entry response over two ranges of projection length ($2 < L/R_p < 3$; $3 < L/R_p < 4$) then taking the mean of the slopes to characterize the flow rate. The average flow rate was then scaled by the corresponding excess pressure. Fig. 5 presents the cumulated results from analysis of each cell entry flow test by this procedure at low excess suction (2–4× threshold). Fig. 6 presents results for cells aspirated at the higher excess suction (20–30× threshold). The data in Figs. 5 and 6 are organized to demonstrate the behavior of each

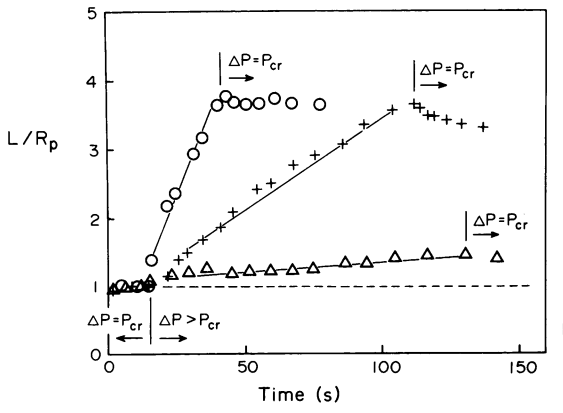

FIGURE 4. Measurements of projection length versus time for a single granulocyte subjected to three aspiration tests with a medium-size pipet where suction pressure was varied between 1.5–4.3 times the threshold value. This figure illustrates the proportional increase in entry flow rate with excess pressure above the threshold value.

granulocyte in the four aspiration tests as follows: data for the two values of suction applied with a single pipet are denoted by an open circle (o) for the upper pressure and a cross (x) symbol for the lower pressure connected by a vertical line. Each set of four measurements is connected by a line between midpoints of the two vertical lines (for upper/lower pressures) to identify a single cell tested with two pipets. Typical of mechanical responses of biological cells, there is considerable scatter in the data. However, the scaled entry rates for a given ratio of pipet caliber to cell diameter show no systematic correlation with excess pressure which would reflect non-Newtonian behavior.

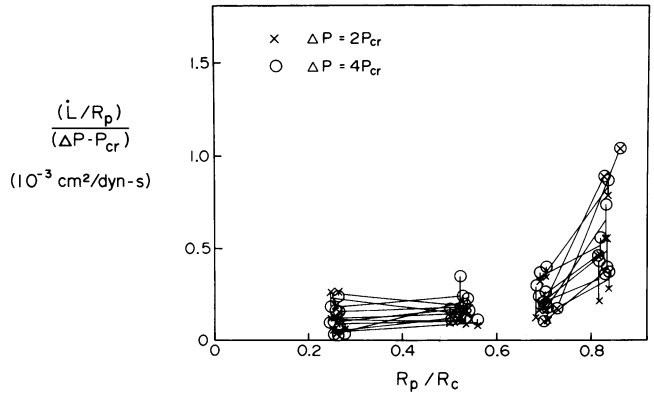

FIGURE 5. Average entry flow rates ($\dot{L}/R_p$) scaled by the excess pressure versus pipet size to cell size ration for low suctions (2–4× threshold). The results represent four aspiration tests on each granulocyte as follows: data for two values of suction applied with a single pipet are denoted by an open circle (O) for the upper pressure and a cross (x) for the lower pressure connected by a vertical line; each set of four measurements is connected by a line between midpoints of the two vertical lines (for upper/lower pressures) to identify the same cell.

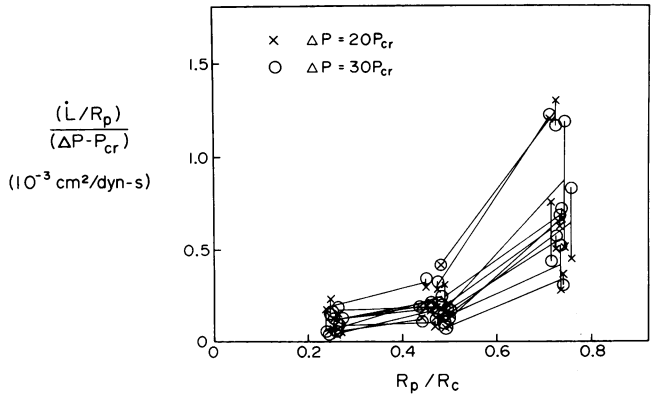

FIGURE 6. Average entry flow rates ($\dot{L}/R_p$) scaled by excess pressure for the higher suction range (20–30× threshold) versus pipet size to cell size ratio. The results represent four aspiration tests on each granulocyte as follows: data for two values of suction applied with a single pipet are denoted by an open circle (O) for the upper pressure and a cross (x) for the lower pressure connected by a vertical line; each set of four measurements is connected by a line between midpoints of the two vertical lines (for upper/lower pressures) to identify the same cell.

Most likely, variations reflect fluctuations in cell state. Furthermore, the near Newtonian character of the entry flow is clearly demonstrated by noting that data in Fig. 5 for scaled flow rates measured at low excess suction 2–4× threshold) are comparable to the data in Fig. 6 for scaled flow rates produced by excess suctions which were an order of magnitude larger (20–30× threshold).

Based on the continuous flow observed for suctions in excess of the threshold and assuming a Newtonian-like proportionality between flow and excess suction, the results in Figs. 5 and 6 were correlated with the cell model of a liquid core encapsulated by a cortical gel layer. Analysis of this model (9), showed that entry flow rate scaled by excess suction depends on two parameters: the effective viscosity μ of the liquid core and a dimensionless ratio $\tilde{\eta}$ that represents the contribution of viscous resistance in the cortical layer to the total viscous resistance to entry. The model predicts that augmentation of viscous flow resistance by dissipation in the cell cortex should be more pronounced for flow into small pipets than into large pipets. Thus, an estimate of the dimensionless ratio $\tilde{\eta}$ can be obtained by correlation of the theoretical prediction with measured values for flow resistance. Fig. 7 presents the average flow resistance and standard deviation of all tests with a single pipet size versus the pipet radius to cell radius ratio (from data given in Figs. 5 and 6). Values are plotted in Fig. 7 with an unfilled triangle (△) for the lower suction range (2–4× threshold) and with a filled triangle (▲) for the higher suction range (20–30× threshold). Also shown in Fig. 7 are theoretical predictions of flow resistance that demonstrate the effect of dissipation in the cortical layer over a two order of magnitude range in $\tilde{\eta}$.

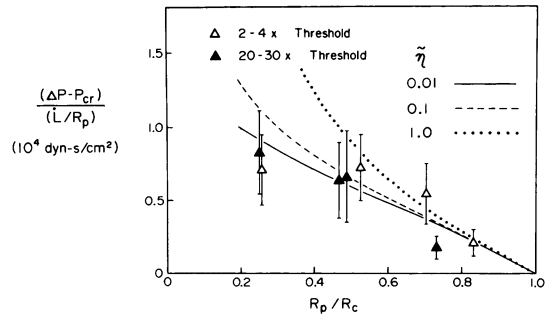

FIGURE 7. Correlation of theoretical predictions for flow resistance of a liquid-like model cell into different-size tubes with values of entry flow resistance measured in the pipet tests. Mean experimental values are plotted with an unfilled triangle (△) for the lower suction range (2–4× threshold) and with a filled triangle (▲) for the higher suction range (20–30× threshold); brackets about the mean values represent ±1 SD in the measured values of flow resistance. The theoretical curves were calculated for a two order of magnitude range in characteristic parameter $\tilde{\eta}$, which represents the ratio of cortical flow resistance to that of the liquid core: μ = 1,700 poise for $\tilde{\eta}$ = 1.0; μ = 2,000 poise for $\tilde{\eta}$ = 0.1; μ = 2,000 poise for $\tilde{\eta}$ = 0.01. From this comparison, a value of $\tilde{\eta}$ = 0.01 was chosen to represent the characteristic ratio of dissipation in the cortex to that interior to the cell.

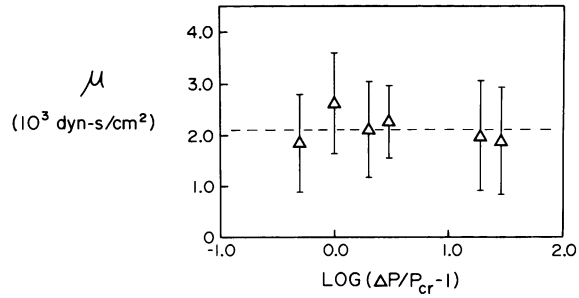

FIGURE 8. Values of apparent cell viscosity for each cell measurement (based on the theoretical prediction of dimensionless flow resistance) versus the logarithm of the ratio of the excess pressure to the threshold pressure. The cortical dissipation parameter $\tilde{\eta}$ was taken as 0.01. The range of excess suction to threshold pressure ratio represents a range of shear rate from 0.02 to 3.0 s^{-1}. The average value of the apparent cell viscosity for all measurements is 2.1 ± 1 × 10^3 poise (dyn-s/cm^2) for these measurements at 23°C.

Even with the large variance in the data, the results clearly show that dissipation in the liquid core dominates the entry flow resistance and that dissipation in the cortical layer is small. It is important to note that even though small, dissipation in the cortex cannot be neglected and is predicted to be significant for small size pipets (9). However, this feature is difficult to confirm accurately with small pipets (≳2 μm) because the coarse structure of the cell interior interferes with entry into the tube. The results in Fig. 7 correlate best with predictions for flow resistance based on a cortical dissipation parameter of $\tilde{\eta}$ = 0.01. With this value for $\tilde{\eta}$, it is possible to calculate the apparent viscosity for each cell measurement from the predicted value of dimensionless flow resistance $(\Delta P - P_{cr})/\mu(\dot{L}/R_p)$ for the appropriate ratio of pipet radius to cell radius. Fig. 8 is the plot of apparent cell viscosities calculated from the measured flow resistances versus excess suction divided by the threshold pressure. As seen in Fig. 8, there is no obvious dependence of viscosity on suction pressure and therefore shear rate; however, a weak dependence could exist that would not be discernible from the scatter in cell properties.

The apparent viscosity of granulocytes derived from the values shown in Fig. 8 is 2.1 ± 1 × 10^3 poise (dyn-s/cm^2) determined from tests at 23°C. Similar entry flow tests on single cells with a single pipet (~4 μm caliber) were carried out at three other temperatures (10°, 15°, 37°C) to determine the temperature dependence of the apparent cell viscosity. Based on the measured entry flow resistance (excess suction divided by entry flow rate) and the pipet to cell size ratio, the apparent viscosities at these temperatures were obtained by similar correlation with the theoretical prediction for flow resistance again with a value of $\tilde{\eta}$ = 0.01. Fig. 9 presents the results for apparent cell viscosity versus temperature.

CONCLUSIONS

Aspiration of single granulocytes into micropipets with sizes that ranged from 0.25 to 0.8 times the cell diameter showed that cells behaved passively as liquid-like bodies for suction pressures in excess of a threshold pressure. Measured threshold pressures correlated with values predicted for a persistent cortical tension of 0.035 dyn/cm. When suction exceeded the threshold, continuous flow

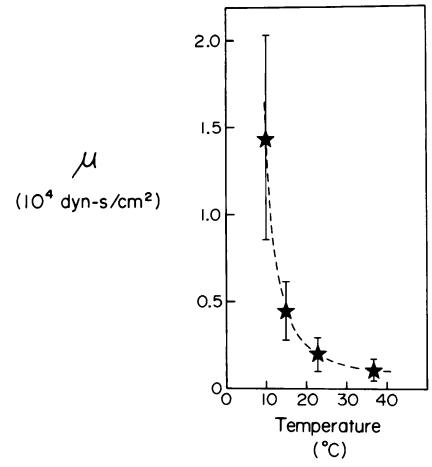

FIGURE 9. Apparent cell viscosity as a function of temperature.

would lead to total aspiration of passive cells into pipets with calibers >2.7 μm. For pipet sizes <2.7 μm, there was a maximum projection length to which cells could be aspirated, beyond that length lysis occurred. These maximal extensions were consistent with elimination of wrinkles and folds in the superficial plasma membrane and when analyzed as such gave values of surface excess (above the area necessary to cover the initial spherical volume) in the range of 110–120%. These values were somewhat greater than the estimates of 84% derived from sophisticated morphometric analyses in the past (10). With pipet sizes >2.7 μm, four continuous flow tests (at constant suction) were carried out with two different size pipets on individual cells. From these tests, measurement of entry flow resistance (excess pressure divided by rate of entry) showed that flow resistance was dominated by the cytoplasmic core of cells. Based on correlation with an idealized model of the cell as a liquid core encapsulated by a viscous cortical shell, the characteristic parameter for ratio of dissipation in the cortex to the cell interior appeared to be small and on the order of 0.01 in magnitude. Calculations of apparent cell viscosity from each cell test were made with the predicted values for dimensionless flow resistance at each pipet to cell size ratio and with the measured values of flow resistance. The calculated values of apparent viscosity showed no obvious dependence on excess suction pressure which ranged from 2 to 30 times the threshold. At 23°C, the apparent cell viscosity was calculated to be $2.1 \pm 1 \times 10^3$ poise. The characteristic scale of shear rates in these experiments was from 0.02 to 3.0 s^{-1} based on rate of entry divided by pipet radius. For a similar range of shear rate, Valberg and Feldman (2) measured values of $2 - 3 \times 10^3$ poise for viscosity of lung macrophages with a method based on random depolarization of small magnetic particles ingested by cells before polarization by an external magnetic field. It is interesting that the magnetic particle method used by these investigators yields a superposition of local measurements of viscosity (presumably at many positions within the cell) which is nearly identical to that derived here for whole cell flow into tubes. This comparison indicates that both methods give similar averages of viscous dissipation over the cell structure.

In contrast with the large viscosity values found here for continuous flow of granulocytes into pipets, small displacement ($L/R_p \simeq 1$) of granulocytes into pipets over short time intervals has indicated values of viscosity that are 20-fold lower (3, 4). It could be that the lower values of viscosity measured in small displacement tests reflects a much lower level of viscosity in the cortical region. Similarly, we found that the apparent viscosity of granulocytes was a very strong function of temperature whereas small deformation/short time observations (4) has yielded only a weak dependence of viscosity on temperature. The apparent viscosity in our measurements decreased by about a factor of two when the temperature was increased from 23° to 37°C. However, more striking was the increase in viscosity by an order of magnitude when the temperature was lowered from 23° to 10°C. The strong temperature dependence of viscosity is consistent with the retardation observed for engulfment of yeast pathogens by granulocytes at low temperatures (E.A. Evans, manuscript submitted for publication). In fact, the extremely large viscous resistance to motion below 15°C appears to account for the lack of activity of granulocytes at low temperatures.

Our experiments were carried out with low suction pressures ($<10^{-2}$ atmosphere = 10^4 dyn/cm^2) which if held for sufficient periods would yield total aspiration of cells within 1–10 s (longer times for smaller sized pipets and lower pressures). Based on the apparent Newtonian behavior, it is expected that higher pressures in the range of 0.1–1.0 atmosphere would decrease cell entry times by 1 to 2 orders of magnitude to values <1 s/cell. Such large pressures have been used to push white cells through filters (11) and for rapid suction of cells into micropipets (12, 13). In those studies as well as the measurements reported here, flow of single granulocytes in response to applied stresses exhibited a great deal of heterogeneity. Heterogeneity of granulocyte behavior in general appears to be a common feature of these cells (14). The variability observed in flow resistance could be a major factor in the observed irregularities in granulocyte locomotion and phagocytosis.

As mentioned in the Introduction, a different rheological model has been developed by other investigators (3, 4) to represent the short-time, small-deformation response of granulocytes to applied forces. The material concept is based on a representation for a viscoelastic-solid as the action of an ideal elastic element parallel with a Maxwell-liquid (i.e., a simple liquid with a fading elastic response). Hence, three material constants appear in this model: the principal elastic stiffness k_1, which represents an ultimate static-limit to deformation of the cell (i.e., at infinite times, deformation is fixed without flow); an adjacent element with elastic stiffness k_2 (which yields an instantaneous stiffness = $k_1 + k_2$) and a viscous coefficient μ. After the initial elastic response at $t = 0$ to a step force, the transient rate of deformation is represented by a time constant $t_r = \mu(k_1 + k_2)/k_1k_2$. Because the response is transient, the time constant also indicates the period of time required to approach a static equilibrium (~2–3 t_r). Thus, the general prediction of this viscoelastic-solid model is quite different from that represented by the liquid core-cortical tension model we have proposed (1, 9): i.e., the solid body approaches a fixed deformation at long times whereas the liquid-like model continues to flow. Recovery after deformation to the original spherical

form is assured by both models but through different mechanisms. In the viscoelastic-solid model, the parallel-elastic stiffness k_1 creates restoring forces throughout the cell in proportion to deformation. On the other hand, the cortical tension in the liquid core model localizes persistent restoring forces in the surface region. As we will discuss, these two types of restoring forces can yield the same apparent time for recovery after deformation with markedly different values for viscous coefficients because of the difference in mechanisms. First, it is important to describe the general features of the viscoelastic-solid model in the context of experimental observations and to review the values published for the coefficients (k_1, k_2, μ) as granulocyte properties.

The viscoelastic-solid model has primarily been correlated with the initial displacement response of white cells in pipet aspiration tests ($L/R_P \sim 1$ or less) which typically represents a range from 0 to 2 s. As such, the exponential-like response has been fitted to a function that is only slightly nonlinear (see 3, 4, 15, 16). A wide variety of values have been published to represent average properties of granulocytes: e.g., $k_1 = 56$ dyn/cm^2, $k_2 = 600$ dyn/cm^2, $\mu = 96$ dyn-s/cm^2 (reference 3); $k_1 = 275$ dyn/cm^2, $k_2 = 737$ dyn/cm^2, $\mu = 130$ dyn-s/cm^2 (reference 15); $k_1 = 7.5$ dyn/cm^2, $k_2 = 238$ dyn/cm^2, $\mu = 330$ dyn-s/cm^2 (reference 16). These sets of coefficients predict characteristic response times of $t_r = 1.8$, 0.65, and 45 s, respectively. Hence, the values predict that granulocytes should flow into pipets with a strongly nonlinear response and should appear to stop after a few seconds in the first two cases or after a couple of minutes in the latter case. Certainly, this is not the observed behavior as shown in Fig. 4. In addition, the viscoelastic-solid behavior predicts that the threshold pressure (required to keep the cell extended without flow) should increase with the length of the cell aspirated into the pipet; thus, when the suction pressure is returned to the initial level P_{cr}, the cell should recover to a length equal to the pipet radius. Again, this prediction is not consistent with the behavior observed in Fig. 4. The unavoidable conclusion is that the parallel-elastic stiffness in the viscoelastic-solid model cannot represent the cell response for more than a short-time period except when extensions into the pipet are less than one radius. On the other hand, the elastic stiffness in series with the viscous element leads to a slight Maxwell-type liquid response (a fading memory) which is clearly apparent in Fig. 4 (i.e., the small recoil when the suction pressure is returned to the threshold level after the period of flow). As shown in Fig. 4, this is not a dominant feature of cell response and recovery. The large values of k_2 found with the viscoelastic-solid model also indicate that this component does not greatly affect the response and recovery times.

What appears puzzling is the major difference between viscosities found for granulocytes in our experiments ($\sim 2 \times 10^3$ dyn-s/cm^2) and by Valberg et al. (2) with different methods compared with those published for the viscoelastic-solid model ($\sim 1 - 3 \times 10^2$ dyn-s/cm^2). However, this difference can be understood in terms of the nature of the elastic restoring forces in each model. The simplest way to evaluate the nature of each model is to examine the force-free recovery of a cell after deformation. For this purpose, rapid release of granulocytes after large extensions into micropipets has been studied to obtain estimates of characteristic times for recovery (1, 16). Based on the initial rates of recovery, characteristic values for time constants were found to be in the range of 20–30 s. Detailed analysis of recovery from totally-aspirated sausage shapes to spheres have been carried-out for both the viscoelastic-solid model and a liquid-like model with a cortical tension (17). In fact, the last set of properties referred to above for the viscoelastic-solid model (which gave the large time constant -45 s) were determined from analysis of this type of experiment. In the correlation of the viscoelastic-solid model with experiment, it was recognized that the magnitude of the parallel elastic coefficient k_1 had to be drastically reduced and the viscous coefficient μ increased in order to match the long-term recovery phase. For comparison, the authors also computed the recovery behavior for a liquid-like cell with the same Maxwell-liquid properties (i.e., $\mu = 300$ dyn-s/cm^2 and $k_2 = 285$ dyn/cm^2) but with a cortical tension of 0.031 dyn/cm to replace the parallel-elastic element (17). However, there was an obvious discrepancy between predictions of the recovery phase between the viscoelastic-solid model (16) and the liquid-like core model (17) for the same level of viscosity. Here, the recovery predicted for the Maxwell-liquid core model was about a factor of six faster than for the viscoelastic-solid model. Clearly, to achieve the same time course for recovery, the viscosity in the liquid core-cortical tension model would have to be increased to a value comparable with that found here (and by Valberg et al., $\sim 2 \times 10^3$ dyn-s/cm^2). The explanation is simple. With the liquid core model, the initial rate of recovery is driven by the differential normal stress on the liquid surface between the poles and the equator of the sausage form. Based on the difference between the curvatures of the spherical ends and the cylindrical equator, the initial magnitude of this deviatioric stress will be on the order of the cortical tension divided by the radius, i.e., $\bar{\tau}_o/R$. Thus, the characteristic recovery time is of order $t_r \sim \mu R/\bar{\tau}_o$. As such, viscosity values of 2×10^3 dyn-s/cm^2 and tension values of 0.035 dyn/cm (found here) would predict recovery times on the order of 20 s consistent with experimental observations. Further, to predict equal values of initial recovery rates with both liquid core and viscoelastic-solid models, the viscous coefficients would be related approxi-

mately by the ratio $\bar{\tau}_o/(k_1 R) \sim 10$ which appears to account for the different viscosity values obtained with each model.

In summary, a Maxwell-liquid subject to a persistent cortical tension appears to be the most realistic model for entry-flow produced by pipet suction forces and for the force-free recovery after large deformation of passive granulocytes. When the fading elastic response (recoil) is small (as indicated in Fig. 4 after the pressure is returned to P_{cr}), then the behavior can be predicted by simple superposition of either an instantaneous length increment in response to a step-increase in pressure or an exponentially-decaying increment after a step-reduction in pressure. For such linear response, it has been shown (3) that the behavior can be derived simply from the entry flow rate of the pure liquid model multiplied by an appropriate history function which involves a characteristic decay time equal to μ/k_2. However, for continuous entry flow at constant suction pressure ($>P_{cr}$), the flow rate is determined only by viscosity for this level of approximation.

The authors acknowledge the expert technical assistance of Barbara Kukan who carried-out the micropipet aspiration tests on granulocytes.

This research was supported by National Institutes of Health grant GM38331.

Received for publication 14 December 1988 and in final form 16 March 1989.

REFERENCES

1. Evans, E. A. 1984. Structural model for passive granulocyte behavior based on mechanical deformation and recovery after deformation tests. *In* White Cell Mechanics: Basic Science and Clinical Aspects. Meiselman, Lichtman, and LaCelle, editors. Alan R. Liss, Inc. New York. 53–71.

   Evans, E. A., and B. Kukan. 1984. Passive material behavior of granulocytes based on large deformation and recovery after deformation tests. *Blood.* 64:1028–1035.

2. Valberg, P. A., and D. F. Albertini. 1985. Cytoplasmic motions, rheology, and structure probed by novel magnetic particle method. *J. Cell Biol.* 101:130–140.

   Valberg, P. A., and H. A. Feldman. 1987. Magnetic particle motions within living cells: measurement of cytoplasmic viscosity and motile activity. *Biophys. J.* 52:551–561.

3. Schmid-Schonbein, G. W., K. L. P. Sung, H. Tozeren, R. Skalak, and S. Chien. 1981. Passive mechanical properties of human leukocytes. *Biophys. J.* 36:243–256.

4. Sung, K. L. P., G. W. Schmid-Schonbein, R. Skalak, G. B. Schuessler, S. Usami, and S. Chien. 1982. Influence of physiochemical factors on rheology of human neutrophils. *Biophys. J.* 39:101–106.

5. Southwick, F. S., and T. P. Stossel. 1983. Contractile protein in leukocyte function. *Semin. Hematol.* 20:305–321.

6. Stossel, T. P., J. H. Hardwig, H. L. Yin, and O. Stendahl. 1980. The motor of amoeboid leukocytes. *Biochem. Soc. Symp.* 45:51–63.

7. Oliver, J. M., and R. D. Berlin. 1983. Surface and cytoskeletal events regulated leukocyte membrane topography. *Semin. Hematol.* 20:282–304.

8. Valerius, N. H., O. Stendahl, J. H. Hardwig, and T. P. Stossel. 1981. Distribution of actin-binding protein and myosin in polymorphonuclear leukocytes during locomotion and phagocytosis. *Cell.* 24:195–202.

9. Yeung, A., and E. Evans. 1989. Cortical shell-liquid core model for passive flow of liquid-like spherical cells into micropipets. *Biophys. J.* 56:139–149.

10. Schmid-Schonbein, G. W., Y. Y. Shih, and S. Chien. 1980. Morphometry of human leukocytes. *Blood.* 56:866–875.

11. Lichtman, M. A., and E. A. Kearney. 1976. The filterability of normal and leukemic human leukocytes. *Blood Cells (Berl.).* 2:491–506.

12. Lichtman, M. A., and R. I. Weed. 1972. Alteration of the cell periphery during granulocyte maturation: relationship to cell function. *Blood.* 39:301–316.

13. Miller, M. E., and K. A. Myers. 1975. Cellular deformability of the human peripheral blood polymorphonuclear leukocyte: method of study, normal variation and effects of physical and chemical alteration. *Res. J. Reticuloendothel. Soc.* 18:337–345.

14. Gallin, J. I. 1984. Human neutrophil heterogeneity exists, but is it meaningful? *Blood.* 63:977–983.

15. Chien, S., G. W. Schmid-Schonbein, K.-L. P. Sung, E. A. Schmalzer, and R. Skalak. 1984. Viscoelastic properties of leukocytes. *In* White Cell Mechanics: Basic Science and Clinical Aspects. Alan R. Liss, Inc, New York. 19–51.

16. Sung, K.-L.P., C. Dong, G. W. Schmid-Schonbein, S. Chien, and R. Skalak. 1988. Leukocyte relaxation properties. *Biophys. J.* 54:331–336.

17. Dong, C., R. Skalak, K.-L. P. Sung, G. W. Schmid-Schonbein, and S. Chien. 1988. Passive deformation analysis of human leukocytes. *J. Biomech. Eng.* 110:27–36.